Talanta 81 (2010) 908–915

Contents lists available at ScienceDirect

Talanta

journal homepage: www.elsevier.com/locate/talanta

Conductive bio-Polymer nano-Composites (CPC): Chitosan-carbon nanotube transducers assembled via spray layer-by-layer for volatile organic compound sensing

Bijandra Kumar, Jean-François Feller*, Mickaël Castro, Jianbo Lu

Smart Plastics Group, European University of Brittany (UEB), LIMAT^{B}-UBS, Lorient, France

ARTICLE INFO

Article history:
Received 7 November 2009
Received in revised form
26 December 2009
Accepted 17 January 2010
Available online 25 January 2010

Keywords:
Conductive bio-Polymer nano-Composites (CPC)
Chitosan
Carbon nanotube (CNT)
Solvent vapour sensing
AFM
E-nose

ABSTRACT

The chemo-electrical properties of chitosan-carbon nanotubes (Chit-CNT) Conductive bio-Polymer nano-Composites (CPC) transducers processed by spray layer-by-layer (LbL) technique have been investigated. Results show that unlike most synthetic polymer matrices, chitosan provides the transducer with high sensitivity towards not only polar vapours like water and methanol but also to a lesser extent toluene. Quantitative responses are obtained, well fitted with the Langmuir-Henry-Clustering (LHC) model allowing to link electrical signal to vapour content. Chit-CNT transducers selectivity was also correlated with an exponential law to the inverse of Flory–Huggins interaction parameter χ_{12}. These properties make Chit-CNT a good transducer to be implemented in an e-nose. Additionally, the observation by atomic force microscopy (AFM) of Chit-CNT morphology suggests a chemical nano-switching mechanism promoting tunnelling conduction and originating macroscopic vapour sensing.

1. Introduction

Advances in nanotechnology and evolution of new smart materials have been playing a key role in the development of very accurate and reliable sensors [1]. Particularly carbon nanotubes since their discovery [2] have shown many exceptional mechanical [3], electromechanical [4] and electrical [5,6] properties, which allowed many new applications [7,8]. Carbon nanotube based materials have also proved their high potential for smart applications such as flow sensing [9], chemical sensing [10,11], biosensing [12,13] or cancer diagnosis and treatment [14,15]. Conductive bio-Polymer nano-Composites (CPC) obtained by percolating [16,17] conducting nanofillers (metal or carbon) into an insulating polymer matrix have also shown high sensitivity towards temperature variations [18–24], biomolecules in solution [25], organic volatile compound in atmosphere [26–35]. Their ability to transduce this information into interpretable signals made them crucial components of electronic noses (e-nose) [36–39], which were popularized by NASA to detect organic vapours leaks in space shuttles [40–42]. Nevertheless, there is no doubt that these already very effective smart devices will see the number of their applications quickly increasing due to both the discovery of new targets such as lung cancer anticipated diagnosis by analysis of exhaled breath of patients [43] or explosives traces [44,45] and the development of new CPC transducers with hierarchical architectures [46–49] or the use of functionalised nanofillers [50–53]. Molecular recognition of e-noses is not based on a "key/locker" principle because there is generally no univocal relationship between one CPC formulation and one analyte. By mimicking mammalian sense of olfaction e-noses analyse a combination of electrical responses from a set of selected CPC sensors [38,40,43]. The great advantage of this strategy compared to traditional molecular recognition is to allow the detection of an unknown molecule provided that the e-nose has "learnt" to sense typical vapours. Thus the accuracy of the nose will depend on quality of both calibration and assortment of its elementary CPC transducers. Consequently CPC based e-noses selectivity and sensitivity can still be improved taking benefit from new developments in the CPC field. Firstly, although few studies report the use of CPC matrices sensitive to water vapour like poly(ethylene terephthalate) [54], poly(ethylene-co-vinyl acetate) [27] or poly(vinyl alcohol) [26], it is possible to overcome the lower sensitivity of sensors to polar vapours like water and methanol by using hydrophilic natural polymer matrices like chitosan [35]. In fact, chitosan is also very attractive because of its biocompatibility, biodegradability, and bioactivity used for many applications in medicine, pharmacy, etc. [55–58]. Secondly, the implementation of

* Corresponding author. Tel.: +33 297 874 584; fax: +33 297 874 588.
E-mail address: jean-francois.feller@univ-ubs.fr (J.-F. Feller).

0039-9140/$ – see front matter © 2010 Elsevier B.V. All rights reserved.
doi:10.1016/j.talanta.2010.01.036

Table 1
Chemical structure and physical properties of chitosan.

Chitosan (molecular structure)	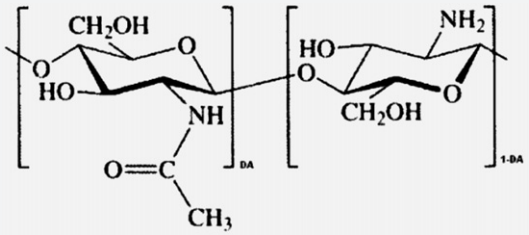
Molecular weight	190,000–310,000 g mol^{-1}
Degree of acetylation DA	15–25%
Index of secondary swelling in water WRV	104%
Ashe	0.26%
Humidity	2.74%
Viscosity	86.4 Pa.s (20 °C, 30 rmp)

carbon nanotubes (CNT) in polymer matrices apart from improving mechanical properties [59] or electrical conductivity [60] has also proved to be effective in designing electrochemical [61–66] and amperometric [67] biosensors especially when associated to chitosan. All these considerations suggest that combining CNT with a biomatrix such as chitosan will provide effective transducers for e-noses although to our knowledge there is no report in literature of any use of Chit-CNT to sense organic vapours.

To investigate this new idea, we have developed Chit-CNT transducers hierarchically structured by spray layer-by-layer on microelectrode using a newly developed protocol [49] and then studied their chemo-electrical properties by submitting them to a set of typical solvent vapours. Results are analysed with the Langmuir-Henry-Clustering (LHC) model [35] and interpreted in the light of CPC morphology at the nanoscale determined by atomic force microscopy (AFM), and also considering χ_{12} the Flory–Huggins intermolecular interactions parameter.

2. Experiments

2.1. Materials

N-7000 multiwall carbon nanotubes (CNT), kindly provided by Nanocyl® (Belgium) were dried under vacuum at 60 °C temperature for 24 h prior to solution preparation. According to TEM data of the producer, this grade corresponding to CNT with an average diameter of 10 nm and a mean length between 100 and 1000 nm, is in good agreement with AFM measurements of this paper. Chitosan (Chit) which is a random copolymer made of β-(1→4)-N-acetyl-D-glucosamine and a-(1→4)-D-glucosamine was purchased by Aldrich (France). Some of its characteristics such as molecular weight and degree of acetylation (DA) are presented in Table 1. Decreasing chitosan DA under 50% by partial deacetylation of chitin (poly-β-(1→4)-N-acetyl-D-glucosamine), results in a higher solubility in aqueous media which also facilitates CNT dispersion and transducers processing. All solvents (water, methanol and toluene) were obtained from (Aldrich, France) and used as received.

2.2. Fabrication of vapour sensors

Fabrication of vapour sensors was performed in two steps. Firstly 20 mg of chitosan were dissolved in 1% acetic acid solution at 50 °C temperature under constant stirring. After obtaining a clear solution, the desired amount of carbon nanotubes (in vol.%) was dispersed under sonication for 1 h at 50 °C and kept degassing for 30 min once a homogeneous Chit-CNT dispersion was achieved. In a second step, CPC transducer films were processed by spray deposition layer-by-layer (LbL) technique [30–33] onto inter-digitated electrodes composed of 25%Ag/75%Pd tracks separated by 15 μm ceramic gap and prepared by cleaving 22-nF capacitors [37]. Electrodes were polished and then cleaned with ethanol to remove any pollution from their surface. CPC solution was sprayed onto electrodes layer-by-layer with a homemade device allowing a precise control of nozzle scanning speed (V_s = 10 cm s^{-1}), solution flow rate (index 2), stream pressure (p_s = 0.20 MPa), and target to nozzle distance (d_{tn} = 8 cm). During solvent evaporation, CPC micro beads of 50–100 nm can weld to form a hierarchical 3D networks by percolation [49]. Transducer film thickness was kept constant by spraying ten layers for all samples to ensure a good reproducibility of dynamic properties of sensors. After fabrication, vapour sensors were conditioned at 30 °C in controlled atmosphere for one night.

2.3. Morphological characterization by AFM

AFM experiments were performed under ambient conditions using light tapping mode AFM (TM-AFM) on a multimode scanning probe microscope (Nanoscope IIIa, Veeco). The ratio of the set point amplitude to the free amplitude was maintained approximately at 0.9. RTESP AFM tips (Veeco), with typical resonance frequency between 300 and 400 kHz and tip radius between 5 and 15 nm were used. Three-dimensional characteristics of CNT as well as Chit-CNT CPC were quantitatively measured using the section analysis software of the microscope (V6.13r1 by Digital instruments). Both curvature and the surface roughness (0.5–1 μm) of films sprayed on inter-digitated electrodes have prevented direct observation by AFM in good conditions; thus, it was necessary to prepare new Chit-CNT films, using the same spray LbL protocol, but this time on silica wafers (Mat. Technology, France) washed with deionised water to remove any contamination and dried with filtered nitrogen. To determine the initial structure of CNT network within CPC, all AFM measurements were done on samples, which had not been exposed to vapours.

2.4. Dynamical vapour sensing measurement

The vapour sensing characteristics of the composites were investigated by recording their chemo-electrical responses when submitted to successive 10 min rectangular pulses of volatile organic compound (VOC) and pure nitrogen flows. Mass flow controllers, solvent bubblers, and a program developed under LabView software drove electrical valves. The organic vapour concentration in the main flow is adjusted by blending two gas streams, one fully saturated through bubblers and another of pure nitrogen. The device is regulated at room temperature. Total flow rate was kept constant during measurement (100 cm^3 min^{-1}). CPC electrical

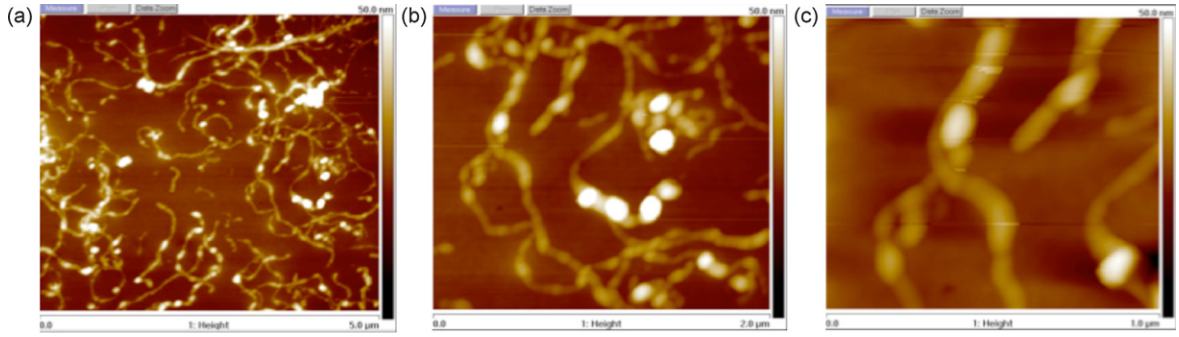

Fig. 1. AFM images (height profile) of Chit-2%CNT (vol.%) CPC from low magnification to high magnification (a) 5 μm, (b) 2 μm and (c) 1 μm full scale successively.

characteristics were recorded with a KEITHLEY 6517A multimeter. The whole device is fully described in a previous paper [53]. Only "fresh" transducers, fabricated in the same conditions, where exposed to the different vapours.

3. Results and discussion

3.1. Chemical switching at the nanoscale

AFM is a versatile technique widely used in nanotechnology to characterize changes in nanotubes morphology occurring at the nanoscale due to any physico-chemical treatment or chemical reaction such as in situ polymerization or grafting on the surface [50–53]. AFM can also be used to manipulate CNT sheathed with poly(carbonate) which have been extracted from a fractured surface in order to visualize their morphology in situ by SEM [68]. More generally as CNT tend to associate into clusters or bundles due to van der Waals forces, AFM is used to determine their aggregation level, after synthesis or after dispersion into solvents or polymer matrices. In this work AFM has been used to visualize pristine CNT structure, after it has been dispersed into chloroform and deposited onto freshly cleaved mica by spin coating at 2500 rpm. Due to the lack of solubility of untreated CNT, several minutes of sonication were necessary to reach a satisfying level of dispersion, immediately prior to spin-coating deposition. On the other hand various surfactants can be used to get individual dispersion of CNT in aqueous solution. Chitosan acting as a cationic surfactant in acidic aqueous solution can be used to achieve a stable dispersion of CNT leading to several advanced applications [62,69,70]. AFM experiments have also been performed to determine the actual morphology of Chit-CNT transducers, and its influence on chemo-electrical properties. A homogeneous dispersion of CNT was observed for Chit-CNT composites as attested in Fig. 1. It is clearly observed that CNT are well separated from each other and it seems that they are completely coated by chitosan polymer. on Fig. 2 careful observations make it clear that the surface and dimensions of CNT have been considerably modified, evidencing that carbon nanotubes' surface has been fully sheathed by chitosan. From Fig. 3 by comparing dimensional characteristics of pristine CNT and Chit-CNT dimensions, it can be concluded that chitosan chains can pack around CNT to form sheaths about 70–100 nm long and 10–20 nm thick. Moreover, it can be assumed that the same kind of architecture can develop on sensors surface and be the core of the sensing mechanism when penetrant molecules will diffuse through the CPC transducer. Additionally almost no single pristine CNT could be found, whereas the major fraction of the sample was composed of

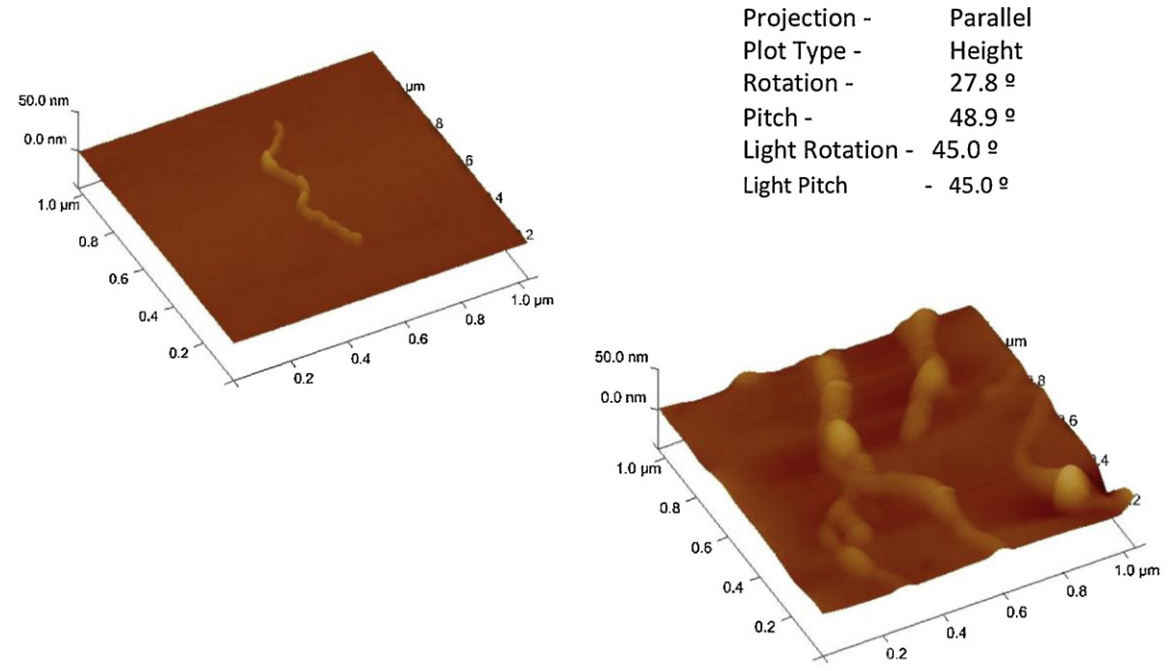

Fig. 2. AFM morphology (height profile) of pristine CNT (left), Chit-CNT (right).

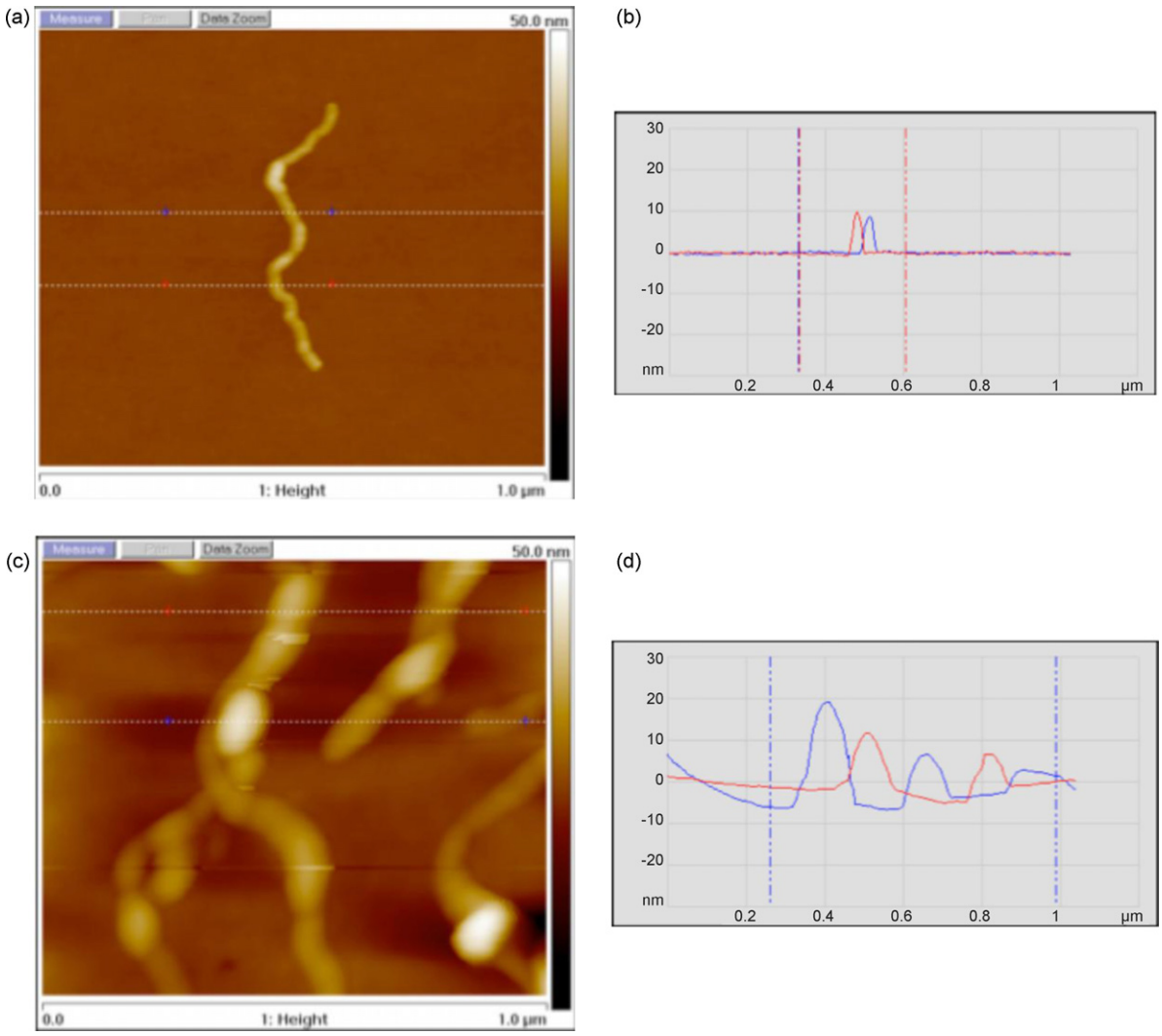

Fig. 3. CNT corrugated by polymer chain (a) pristine CNT and (b) Chit-CNT, with corresponding height curves.

coalesced chitosan coated CNT forming a continuous phase, which could not be easily imaged without damaging AFM tip.

3.2. Chemo-electrical behaviour of Chit-CNT

CPC chemo-electrical response to organic molecules can be interpreted and quantified from the analysis of changes in electrons motion within CNT percolated network. It is assumed that during their diffusion through the composite, vapour molecules can disconnect CNT/CNT junctions by increasing the gap between nanotubes directly by adsorbing on carbon or indirectly by relaxing macromolecules in the vicinity of the junction. Consequently quantum-tunnelling conduction (less effective) will develop to the detriment of ohmic conduction, resulting in an important resistance increase even for a small amount of solvent molecules. The amplitude of this phenomenon is classically evaluated by following the evolution of A_r the relative resistance defined by Eq. (1).

$$A_r = \frac{R_v - R_{init}}{R_{init}} \quad (1)$$

where R_{init} is the initial resistance, R_v the resistance in the presence of vapour. A_r depends on many parameters among which at least the following ones must be controlled: sample thickness (maintained constant in this study by the number of sprayed layers), temperature (controlled around bubblers by thermo-regulated baths and in atmosphere by conditioned air), initial resistance (varied from 2.5 to 18 kΩ by changing CNT content, see Table 2), amount of molecules in the sensor surrounding (varied from 0 to 100% of saturated vapour by accurate flow-meters) and specific interactions of vapour molecules with macromolecules from the matrix (evaluated from solubility parameters available in Table 3 through the determination of Flory–Huggins intermolecular interaction parameters χ_{12} calculated in Table 4). In fact Table 3 shows that not only solubility parameters but also dielectric permittivity and even size of the solvent molecules are different. Nevertheless in the present case they all have a monotonous evolution when ranked according to A_r, which was not the case in a previous study [49]. By changing only one of these influent parameters at the same time it is possible to determine its influence on Chit-CNT sensor chemo-electrical behaviour. In a first experiment only the vapours' nature is changed and electrical responses to water, methanol and toluene are recorded and plotted. Fig. 4 attests the

Table 2
Component compositions for different vapour sensors.

CNT (mg)	Chitosan (mg)	Protonation (%)	CNT (vol.%)	R_{init} (kΩ)
1.76	20	100	2	18
3.54	20	100	4	9.5
5.3	20	100	6	2.5

Table 3
Polarity δ_p, dielectric permittivity ε_r and size d of solvent molecules.

	δ_T ($J^{1/2}\,cm^{-3/2}$)	δ_d ($J^{1/2}\,cm^{-3/2}$)	δ_p ($J^{1/2}\,cm^{-3/2}$)	δ_h ($J^{1/2}\,cm^{-3/2}$)	ε_r ($F\,m^{-1}$)	d (nm)
Water [71]	47.9	15.50	16.00	42.40	75	0.34
Methanol [71]	29.7	15.10	12.30	22.30	32	0.41
Toluene [71]	18.2	18.00	1.40	2.00	2.57	0.575
Chitosan [72,73]	38.61	23.02	17.30	25.72	–	–

Table 4
Global solubility parameters and Flory–Huggins interaction parameters κ_{12} of chitosan with water, methanol and water.

		Water	Methanol	Toluene
Water		–	–	–
Methanol	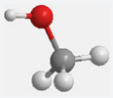	–	–	–
Toluene	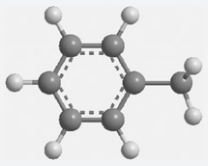	–	–	–
χ_{12}[chitosan]		0.63	1.33	17.92
Ar [Chit-CNT]		0.9	0.3	0.15

efficiency of Chit-CNT to transduce these differences in chemical nature demonstrating at the same time the high selectivity of this sensor towards organic vapours. A_r obtained for water is approximately three times higher than for methanol and five times higher than for toluene. Signals are reproducible from a cycle to the other and no solvent molecules seem to remain inside samples as initial conditions are recovered after full desorption. Although a lower A_r was observed for toluene and methanol, signals were enough well defined to be processed without difficulty. Finally the response times of the different sensors were all of the order of the minute and even less if the first interpretable base line variations are considered.

3.3. Origin of Chit-CNT sensors selectivity

To interpret further on the origin of selectivity of Chit-CNT towards VOC, chemical interactions have been firstly considered. χ_{12} the Flory–Huggins matrix/analyte interaction parameter, already found to be meaningful in interpreting chemo-electrical properties [29], has been calculated with Eq. (2) and collected in Table 4. The closest to zero χ_{12} is, the highest the interactions between polymer chains and organic molecules.

$$\chi_{12} = \frac{V}{RT}(\delta_{T\,pol} - \delta_{T\,sol})^2 \quad (2)$$

With V the molar volume of the solvent ($cm^3\,mol^{-1}$), T: the temperature (K), $R = 8.314\,J\,mol^{-1}$, $\delta_{T\,sol}$: the solvent global solubility parameter ($J^{1/2}\,cm^{-3/2}$), $\delta_{T\,pol}$: the polymer global solubility parameter ($J^{1/2}/cm^{3/2}$), δ_T is derived from Eq. (3)

$$\delta_T^2 = \delta_d^2 + \delta_p^2 + \delta_h^2 \quad (3)$$

where δ_T: global solubility parameter from dispersion bonds between molecules ($J^{1/2}\,cm^{-3/2}$); δ_d: solubility parameter from dispersion bonds between molecules ($J^{1/2}\,cm^{-3/2}$); δ_p: solubility parameter from polar bonds between molecules ($J^{1/2}\,cm^{-3/2}$); δ_H: solubility parameter from hydrogen bonds between molecules ($J^{1/2}\,cm^{-3/2}$).

The following ranking is obtained: χ_{12} (water) < χ_{12} (methanol) < χ_{12} (toluene), which is perfectly correlated with that of response amplitudes: A_r (toluene) < A_r (methanol) < A_r

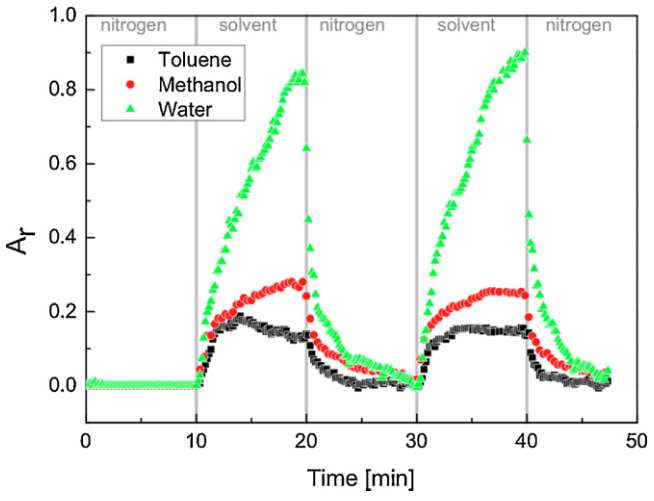

Fig. 4. Response of different vapours towards Chit-2%CNT (vol.%).

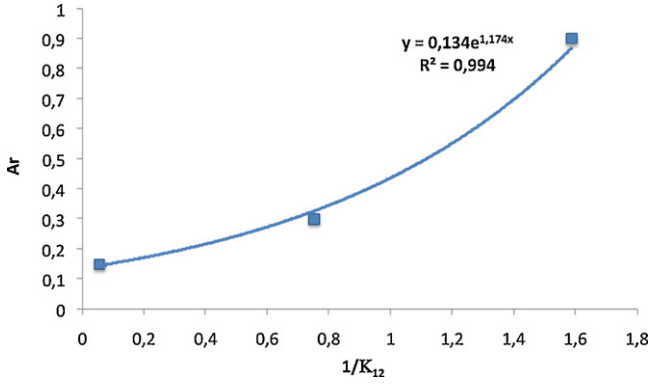

Fig. 5. Correlation between electrical response and molecular interactions.

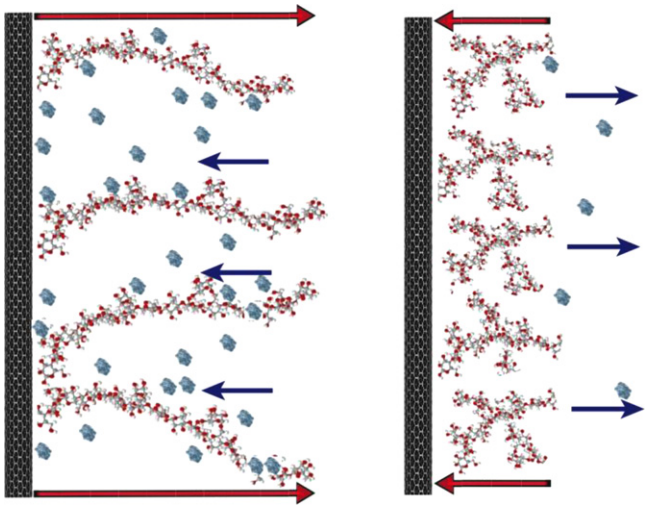

Fig. 6. Schematic drawing of expansion/contraction of chitosan chains during vapour/nitrogen cycles, respectively

(water). As shown in Fig. 5, this correlation is well fitted by Eq. (4) in which A_r increases exponentially with $1/\chi_{12}$.

$$A_r = a\, e^{b/\chi_{12}} \tag{4}$$

where a and b are constants.

This evolution is in good agreement with the results obtained by Yoon et al. [74] who explained this dependency by local volume expansion of the matrix around CNT/CNT junctions. Associating previous statements on chemical interactions with AFM observations of nanotubes wrapped with chitosan macromolecules puts light on what could be the origin of vapour sensing mechanism in CPC: chemical nano-switching resulting from CNT/CNT disjunction due to macromolecules relaxation and further expansion by swelling as schematized in Fig. 6. During organic molecules diffusion, the small gap between CNT (only several nanometers) filled with macromolecule adsorbed on their surface will increase in accordance with the affinity of organic molecules for the polymer matrix. In turn consequences of these structural changes on CPC resistivity will be enhanced due to the fact that tunnelling conduction depends exponentially on inter CNT gap Z according to Eq. (5).

$$\rho = a\, e^{bZ} \tag{5}$$

where ρ is the resistivity, a and b are positive constants and Z is the gap between two vicinal CNT [75].

The sensitivity of final transduction of organic vapour nature/content will thus be proportional to the number of junctions for which $0 < Z < Z_c$, Z_c being the critical gap over which electrons do not have enough energy to jump from a nanotube to the other. In turn the number of chemically switchable junctions will depend on the initial number of junctions related to the amount of CNT in the polymer matrix.

3.4. Effect of initial resistance and CNT content

The best way to investigate the effect of initial number of CNT/CNT junction is to vary the amount of CNT in Chit-CNT to obtain a set of CPC samples with different resistivities as presented in Table 2. This dependency of CPC electrical properties on CNT content simply depends on the percolation theory that describes well the insulator-to-conductor transition in nano-composites observed when increasing conductive filler content [16,17,22,75,76]. At low nanofiller concentrations, the electrical conductivity of the composite remains very close to the conductivity of the pure electrically insulating polymer matrix since the filler amount is not sufficient to form conductive pathways. When a critical filler volume fraction (depending on the nature, size, aspect ratio, compatibility and other factors), called percolation threshold is reached, a three-dimensional conductive network is built through the composite. Table 2 shows that increasing CNT concentration from 2 to 6 vol.% results in a decrease in transducer resistance from 18 to 2 kΩ approximately. When these three different Chit-CNT sensors are exposed to the test set of vapours (water, methanol and toluene), extracting from each experiment the average maximum A_r allows building the graph of Fig. 7. This synthesis provides a good overview of Chit-CNT responses depending on vapour nature and CNT content. Chit-2%CNT is the transducer giving the highest response for all vapours followed successively by Chit-4%CNT and Chit-6%CNT. These results are in good agreement with the percolation theory explaining that the closest the CNT content is to the percolation threshold (estimated 0.5% for Chit-CNT systems) the easiest is the conductive network disconnection and consequently the highest is the variation in magnitude of relative amplitude. Thus the effectiveness of chemical nano-switching due to vapour molecules diffusion is lower for high nanofiller content and in fact Fig. 7 shows that the responses of both Chit-4%CNT and Chit-6%CNT are weak. Additionally, it can be noticed that whatever the CNT content in CPC the vapour ranking is preserved confirming the chitosan selectivity and also reproducibility of experiments.

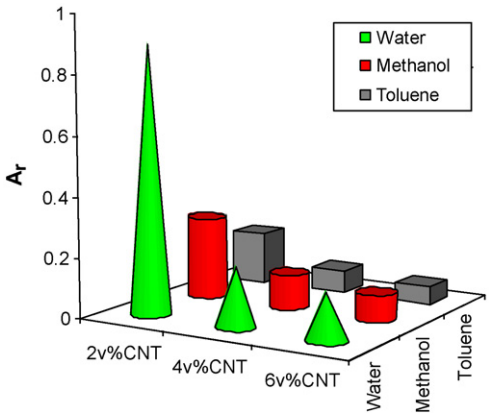

Fig. 7. Effect of CNT concentration on different vapour response.

3.5. Correlation between electrical responses and solvent fraction

Apart from being sensitive to chemical nature of VOC, Chit-CNT sensors can give responses proportional to the amount of organic molecules in their surrounding. Our experimental device allows to scan a wide range of compositions of vapour flows from 0 to 100% (a concentration of 100% corresponds to the saturated vapour). Although with narrow vapour concentration ranges it is convenient for applications to assume a linear evolution, curves of Fig. 8 show clearly that it is not the case on the whole composition range. On the contrary curves for water, methanol and toluene follow quite exactly sorption curves evolution obtained by weight measurement as previously observed [35,49]. Conveniently Chit-CNT sensors chemo-electrical responses are well fitted using the Langmuir-Henry-Clustering (LHC) model [35,53]. This model derived from classical sorption models, describes quite well which diffusion regime takes place in the CPC: simple adsorption, diffusion, clustering, corresponding respectively to the three terms of Eq. (6).

$$A_r = \frac{b_L \cdot (f'' - f) \cdot f}{1 + b_L \cdot f} + k_H \cdot f + (f - f') \cdot f^{n'} \tag{6}$$

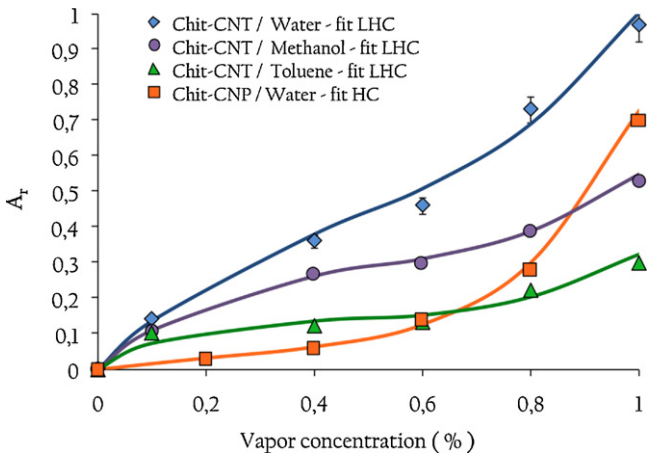

Fig. 8. Influence of vapour concentration on relative amplitude for Chit-2%CNT (vol.%) and Chit-CNP [32] CPC.

where b_L is the Langmuir affinity constant, f' is the vapour fraction over which Langmuir's diffusion is replaced by Henry's diffusion, f is the solvent fraction, k_H is Henry's solubility coefficient, n' the number of vapour molecules associated in clusters.

Moreover, Chit-CNT curves never cross and seem to be homothetic, i.e., their proportionality is the same for all vapour contents. Only the curve of carbon nanoparticles filled chitosan CPC (Chit-CNP) has a different shape: no Langmuir contribution is observed at low vapour concentrations (it can be fitted with only a HC model) and its amplitude is always lower than that of Chit-CNT for the same vapour (water). This result is consistent with the fact that weaker density of junctions is expected in CNT network than in a CNP network. Additionally from being useful to determine the amount of molecules in atmosphere from the electrical response of the CPC, these curves can help to determine the most suitable concentration range for a defined sensor, i.e., they allow to avoid the clustering zone (over 70%) in which the signal can be large but on the other hand can generate non-reversible distortion of the conductive network due to large volume expansion. In fact, solvent molecules meeting the sensor by successive waves will firstly adsorb on macromolecules and CNT without causing much structural changes than simple perturbations of electrons motion. But progressively as their amount in the CPC will increase, carriers will have to jump by tunnelling due to the increasing gap between CNT. Finally in the clustering regime induced by high concentration of water molecules, the expansion of the conducting network results in a sharp increase in CPC resistance. Surprisingly when the sensor is plunged back into pure nitrogen flow, conductive pathways are established again and a quick resistance decrease is observed down to the initial value. This confirms the good stability and durability of Chit-CNT sensors, which is essential for sensing applications.

4. Conclusion

Spray layer by layer has been found to be an effective technique to develop Chit-CNT transducers for vapour sensing. Chitosan matrix has demonstrated a high sensitivity to polar vapours such as water and methanol (difficult to obtain with synthetic polymers being mostly non-polar) but also non polar ones like toluene. This good selectivity on the whole range of vapour content makes Chit-CNT a good candidate for implementation in an e-nose. Interestingly it has been possible to model the evolution of the transducer's response (A_r) with vapour content and to predict its selectivity to vapours as a function of interaction parameter χ_{12}. In light of AFM observations at the nanoscale suggesting how chitosan macromolecules are associated to carbon nanotubes, it was possible to propose a mechanism of chemical nano-switching, which could explain the macroscopic chemo-electrical behaviour of CPC and fits well to the idea that solvent molecules diffusion can lead to an increase of tunnelling conduction.

Acknowledgments

The authors are grateful to Hervé BELLEGOU for his contribution to this work. This research was financed by INTELTEX (Intelligent multi-reactive textiles integrating nanofiller based CPC-fibers), a European Integrated Project supported through the Sixth Framework Program for Research and Technological Development of European Commission (NMP2-CT-2006-026626).

References

[1] V.K. Varadan, K.J. Vinoy, S. Gopalakrishnan (Eds.), Smart Material Systems and MEMS: Design and Development Methodologies, J. Wiley & Sons Ltd., Chichester, England, 2006, pp. 339–340.
[2] S. Iijima, Nature 354 (1991) 56–58.
[3] M.M.J. Treacy, T.W. Ebbesen, J.M. Gibson, Nature 381 (6584) (1996) 678–680.
[4] R.H. Baughmann, C. Cui, A. Zakhidov, Z. Iqbal, J.N. Barisci, G.M. Spinks, Science 284 (1999) 1340–1344.
[5] Z. Yao, C.L. Kane, C. Dekker, Phys. Rev. Lett. 84 (2000) 2941–2944.
[6] M.Q. Ding, W.S. Shao, X.H. Li, G.D. Bai, F.Q. Zhang, Y.H. Li, J.J. Feng, Appl. Phys. Lett. 87 (2005) 233118.
[7] R.H. Baughmann, A.A. Zakhidov, W.A. de Heer, Science 297 (2002) 787–792.
[8] V.N. Popov, Mater. Sci. Eng. R 43 (2004) 61–102.
[9] S. Ghosh, A.K. Sood, N. Kumar, Science 299 (2003) 1042–1044.
[10] J. Kong, N.R. Franklin, C.W. Zhou, M.G. Chapline, S. Peng, K. Cho, H. Dai, Science 287 (2000) 622–625.
[11] J. Li, Y.J. Lu, Q. Ye, M. Cinke, J. Han, M. Meyyappan, Nano Lett. 3 (2003) 929–933.
[12] P.D. Kichambare, A. Star, Nanotechnologies for the Life Sciences, in: C.S.S.R. Kumar (Ed.), Wiley VCH, vol. 8, 2007, pp. 1–26.
[13] J.S. Ye, F.S. Sheu, in: C.S.S.R. Kumar (Ed.), Nanotechnologies for the Life Sciences, Wiley VCH, vol. 8, 2007, pp. 27–55.
[14] K. Shiba, in: C.S.S.R. Kumar (Ed.), Nanotechnologies for the Life Sciences, Wiley VCH, vol. 7, 2007, pp. 285–303.
[15] S.B. Lee, S.J. Son, in: C.S.S.R. Kumar (Ed.), Nanotechnologies for the Life Sciences, Wiley VCH, vol. 7, 2007, pp. 304–337.
[16] S.R. Brodbent, J.M. Hammersley, Proc. Camb. Philos. Soc. 53 (1957) 629–641.
[17] S. Kirkpatrick, Rev. Mod. Phys. 45 (1973) 574–588.
[18] J. Yu, N. Wang, X. Ma, Biomacromolecules 9 (3) (2008) 1050–1057.
[19] I. Mironi-Harpaz, M. Narkis, Polym. Eng. Sci. 41 (2) (2001) 205–221.
[20] C. Wu, S. Asai, M. Sumita, Compos. Int. 49 (2) (1993) 103–106.
[21] Y.H. Hou, M.Q. Zhang, M.Z. Rong, J. Polym. Sci. B 41 (1) (2003) 127–134.
[22] K. Zribi, J.F. Feller, K. Elleuch, A. Bourmaud, B. Elleuch, Polym. Adv. Technol. 17 (9–10) (2006) 727–731.
[23] Y. Xi, Y.Z. Bin, C.K. Chiang, M. Matsuo, Carbon 45 (6) (2007) 1302–1309.
[24] G. Droval, J.F. Feller, P. Salagnac, P. Glouannec, Smart Mater. Struct. 17 (025011) (2008) 1–10.
[25] X.H. Yang, H. Yang, Y.Q. Chen, Q. Yang, L. Wang, 1st Int. Conf. Bioinf. Biomed. Eng., 4272518, 2007, pp. 119–121.
[26] J. Barkauskas, Talanta 44 (1997) 1107–1112.
[27] J.A. Covington, J.W. Gardner, D. Briand, N.F. de Rooij, Sens. Actuators B 77 (1) (2001) 155–162.
[28] J.T. Li, J.R. Xu, M.Q. Zhang, M.Z. Rong, Carbon 41 (2003) 2353–2360.
[29] J.F. Feller, Y. Grohens, Sens. Actuators B 94 (2004) 231–242.
[30] J.F. Feller, Y. Grohens, Synth. Met. 154 (2005) 193–196.
[31] J.B. Schlenoff, S.T. Dubas, T. Farhat, Langmuir 16 (2000) 9968–9969.
[32] A. Izquierdo, S.S. Ono, J.C. Voegel, P. Schaaf, G. Decher, F. Cuisinier, Langmuir 21 (2005) 7558–7859.
[33] K.C. Krogman, N.S. Zacharia, S. Schroeder, P.T. Hammond, Langmuir 23 (2007) 3137–3141.
[34] W. Zeng, M.Q. Zhang, M.Z. Rong, Q. Zheng, Sens. Actuators B 124 (1) (2007) 118–126.
[35] A. Bouvrée, J.F. Feller, M. Castro, Y. Grohens, M. Rinaudo, Sens. Actuators B 138 (2009) 138–147.
[36] M.S. Freund, N.S. Lewis, Proc. Natl. Acad. Sci. U.S.A. 92 (1995) 2652–2656.
[37] M.C. Lonergan, M.S. Freund, E.J. Severin, B.J. Doleman, R.H. Grubbs, N.S. Lewis, Chem. Mater. 8 (9) (1996) 2298–2312.
[38] E.J. Severin, B.J. Doleman, N.S. Lewis, Anal. Chem. 72 (4) (2000) 658–668.
[39] F. Zee, J.W. Judy, Sens. Actuators B 72 (2001) 120–128.
[40] M.A. Ryan, M.L. Homer, M.G. Buehler, K.S. Manatt, B. Lau, D. Karmon, S. Jackson, H. Zhou, Proc. 2nd Int. Conf. Environ. Syst. Soc. Autom. Eng., 1998.
[41] A.V. Shevade, M.A. Ryan, M.L. Homer, A.M. Manfreda, H. Zhou, K.S. Manatt, Sens. Actuators B 93 (2003) 84–91.
[42] M.A. Ryan, H. Zhou, M.G. Buehler, K.S. Manatt, V.S. Mowrey, S.P. Jackson, A.K. Kisor, A.V. Shevade, L. Homer, IEEE Sens. J. 4 (3) (2004) 337–347.

[43] R.F. Machado, D. Laskowski, O. Deffenderfer, T. Burch, S. Zheng, P.J. Mazzone, T. Mekhail, C. Jennings, J.K. Stoller, J. Pyle, J. Duncan, R.A. Dweik, S.C. Erzurum, Am. J. Respir. Crit. Care Med. 171 (2005) 1286–1291.
[44] J.W. Gardner, in: J. Yinon (Ed.), Electronic Noses and Sensors for the Detection of Explosives, Kluwer Pub., Dordrecht, The Netherlands, 2004.
[45] H.M. Briglin, M.C. Burl, M.S. Freund, B.C. Sisk, P. Tokumaru, N.S. Lewis, in: T. Broach, R.S. Harmon, G.J. Dobeck (Eds.) Proc. SPIE 4742 (2002).
[46] L. Zhu, Y. Sun, D.W. Hess, C.P. Wong, Nano Lett. 6 (2006) 243–247.
[47] S.M. Miriyala, Y.S. Kim, L. Liu, J.C. Grunlan, Macromol. Chem. Phys. 209 (23) (2008) 2399–2409.
[48] H.J. Choi, J.Y. Lim, B.J. Park, H.J. Jin, K. Zhang, J. Nanosci. Nanotech. 9 (2) (2009) 1058–1061.
[49] J. Lu, B. Kumar, M. Catro, J.F. Feller, Sens. Actuators B 140 (2009) 451–460.
[50] Z. Yao, N. Braidy, G.A. Botton, A. Adronov, J. Am. Chem. Soc. 125 (2003) 16015–16024.
[51] E. Bekyarova, R.C. Haddon, V. Parpura, in: C.S.S.R. Kumar (Ed.), Nanotechnologies for the Life Sciences, Wiley VCH, vol. 1, 2005, pp. 41–65.
[52] H. Li, F. Cheng, A.M. Duft, A. Adronov, J. Am. Chem. Soc. 127 (2005) 14518–14524.
[53] M. Castro, J. Lu, S. Bruzaud, B. Kumar, J.F. Feller, Carbon 47 (2009) 1930–1942.
[54] K. Parikh, K. Cattanach, R. Rao, D.S. Suh, A. Wu, S.K. Manohar, Sens. Actuators B 113 (2006) 55–63.
[55] M. Rinaudo, Progr. Polym. Sci. 31 (2006) 603–632.
[56] E.R. Welsh, C.L. Schauer, S.B. Qadri, R.R. Price, Macromolecules 3 (2002) 1370–1374.
[57] M.N.V.R. Kumar, R.A.A. Muzzarelli, C. Muzzarelli, H. Sashiwa, A.J. Domb, Chem. Rev. 104 (2004) 6017–6084.
[58] A.J. Varma, S.V. Deshpande, J.F. Kennedy, Carbohyd. Polym. 55 (2004) 77–93.
[59] K.H. Kim, W.H. Jo, Compos. Sci. Technol. 68 (2008) 2120–2124.
[60] S.B. Yang, H.H. Song, X.H. Chen, A.V. Okotrub, L.G. Bulusheva, Electrochim. Acta 52 (2007) 5286–5293.
[61] J.Z. Zhu, Z.Q. Zhu, Z.S. Lai, R. Wang, X.M. Guo, X.Q. Wu, G.X. Zhang, Z.R. Zhang, Y. Wang, Z.Y. Chen, Sensors 2 (2002) 127–136.
[62] M. Zhang, A. Smith, W. Gorski, Anal. Chem. 76 (2004) 5045–5050.
[63] M. Zhang, W. Gorski, J. Am. Chem. Soc. 127 (2005) 2058–2069.
[64] X.L. Luo, J.J. Xu, J.L. Wang, H.Y. Chen, Chem. Commun. 16 (2005) 2169–2171.
[65] X.Q. Cui, C.M. Li, J.F. Zang, S.C. Yu, Biosens. Bioelectron. 22 (12) (2007) 3288–3292.
[66] L. Rassaei, M. Sillanpää, F. Marken, Electrochim. Acta 53 (19) (2008) 5732–5738.
[67] D. Du, X. Huang, J. Cai, A. Zhang, Sens. Actuators B 127 (2) (2007) 531–535.
[68] W. Ding, A. Eitan, F.T. Fisher, X. Chen, D.A. Dikin, R. Andrews, L.C. Brinson, L.S. Schadler, R.S. Ruoff, Nano Lett. 3 (11) (2003) 1593–1597.
[69] V.C. Moore, M.S. Strano, E.H. Haroz, R.H. Hauge, R.E. Smalley, J. Schmidt, Y. Talmon, Nano Lett. 3 (10) (2003) 1379–1382.
[70] Y.Y. Liu, J. Tang, X. Chen, J.H. Xin, Carbon 43 (2005) 3178–3180.
[71] R.H.M. Chan, C.K.M. Fung, W.J. Li, Nanotechnology 10 (15) (2004) 672–677.
[72] J. Brandrup, E.H. Immergut, E.A. Grulke, Polymer Handbook, 4th edition, J. Wiley & Sons, NJ, 1999.
[73] R. Ravindra, Kameswara R. Krovvidi, A.A. Khan, Carbohyd. Polym. 36 (2–3) (1998) 121–127.
[74] H.S. Yoon, J.N. Xie, J.K. Abraham, V.K. Varadan, P.B. Ruffin, Smart Mater. Struct. 15 (2006) S14–S20.
[75] C. Gau, C.Y. Kuo, H.S. Ko, Nanotechnology 20 (395705) (2009) 1–6.
[76] J.F. Feller, S. Bruzaud, Y. Grohens, Mater. Lett. 58 (5) (2004) 739–745.